

# Syntheses and Characterizations of Chiral Tetrahedral Cobalt Phosphates with Zeolite ABW and Related Frameworks

Pingyun Feng, Xianhui Bu, Sarah H. Tolbert, and Galen D. Stucky\*

Contribution from the Department of Chemistry, University of California, Santa Barbara, California 93106

Received October 4, 1996<sup>⊗</sup>

**Abstract:** The hydrothermal syntheses, X-ray crystal structures, and magnetic properties of a family of 3-D chiral framework cobalt phosphates are presented. Two different types of framework structures are described: one has the same topology as the well-known zeolite ABW framework and represents the only pure cobalt phosphate framework with a known zeolite topology; the other exhibits a framework connectivity which can be considered as a hybrid of tridymite and ABW frameworks. These new chiral materials were obtained by systematic chemical variation, accurate control of solution pH values, and use of non-aqueous solvents. Synthesis conditions were found which favored the crystallization of Co<sup>2+</sup> oxygen tetrahedra in strict alternation with P<sup>5+</sup> oxygen tetrahedra from cobalt phosphate solutions in the presence of Na<sup>+</sup>, K<sup>+</sup>, NH<sub>4</sub><sup>+</sup>, or Rb<sup>+</sup> ions. The transition from one framework type to the other is affected by the size of these extra-framework cations. The two ABW structures (NH<sub>4</sub>CoPO<sub>4</sub>-ABW, RbCoPO<sub>4</sub>) have eight-ring channels along the monoclinic *b* axis; the three hybrid hexagonal structures (NaCoPO<sub>4</sub>, KCoPO<sub>4</sub>, NH<sub>4</sub>CoPO<sub>4</sub>-HEX) have six-ring channels along the hexagonal *c*-axis. The 3-D framework of the hexagonal structures is built from a unique [2.2.2]propellane-like triple four-ring unit. Both the ABW framework and the hexagonal framework can be viewed as layers of hexagonal rings directly interconnected by oxygen bridges. The enantiomorphic purity and crystal twinning habits of these materials are correlated with the cation type and synthesis conditions. Magnetic susceptibility measurements at temperatures above 10 K are consistent with pure paramagnetic tetrahedral Co<sup>2+</sup> displaying the Curie–Weiss behavior. At lower temperatures, a ferromagnetic ordering transition is observed with ordering temperatures at or below 3 K.

## Introduction

Aluminosilicate molecular sieves have been extensively studied because of their utility in commercial processes such as catalysis and gas separation.<sup>1</sup> Since the early 1980's, Al<sup>3+</sup> and Si<sup>4+</sup> in the zeolite frameworks have been either completely or partially substituted with a variety of tetrahedral atoms. For example, a number of alumino- (or gallo-) phosphates and zinco- (or beryll-) phosphates or -arsenates have been found to be isotopic with known aluminosilicate molecular sieves.<sup>2,3</sup> Recently, there have been considerable efforts in synthesizing open framework materials with transition metal cations on framework sites. This has resulted in novel framework structures based on vanadium phosphates,<sup>4,5</sup> molybdenum phosphates,<sup>6</sup> *et al.* even though to date no zeolite structure analogs have been reported.

The catalytic applications of cobalt sites in microporous materials have led to many efforts aimed at doping framework structures such as alumino- (or gallo-) phosphates and zinco-phosphates with cobalt ions.<sup>7,8</sup> A number of open framework materials have been reported with cobalt ions partially incorporated into the framework. These include CoAPO-5 and CoAPO-11 which have been used as catalysts in the autoxidation of cyclohexane<sup>9</sup> and *p*-cresol.<sup>10</sup> The recent success in synthe-

sizing zeolite structures such as zeolite-X in the zincophosphate system<sup>2</sup> suggests that it is possible to synthesize microporous structures in the pure cobalt phosphate system. One cobalt phosphate, CoPO<sub>4</sub>·1/2C<sub>2</sub>H<sub>4</sub>(NH<sub>3</sub>)<sub>2</sub>, in which tetrahedral Co<sup>2+</sup> and P<sup>5+</sup> alternate to form an open framework structure with eight-ring channels, has been reported.<sup>11</sup> However, no microporous cobalt phosphate materials with a known zeolite topology have been reported so far.

To achieve a rational design of cobalt phosphate molecular sieves, a logical first step is to start with simple cobalt phosphate salts and study the structural analogies between cobalt phosphate salts and those of aluminosilicates. Being aware that the tremendous success with the aluminophosphate system was in part due to the initial recognition of structural analogies between AlPO<sub>4</sub> and SiO<sub>2</sub>,<sup>12</sup> we seek to determine if the same analogies between AlPO<sub>4</sub> and SiO<sub>2</sub> also exist between cobalt phosphate structures and aluminosilicate minerals. The results would serve as a useful guide on the design of microporous cobalt phosphate frameworks.

An examination of cobalt phosphate salts indicates that there are very few similarities between the structures of known cobalt phosphate salts and aluminosilicate minerals.<sup>13</sup> Unlike aluminosilicates, in which the Si/Al ratio can adopt a variety of values greater than or equal to one,<sup>14</sup> a strict alternation of Co<sup>2+</sup> and P<sup>5+</sup> tetrahedra is required to form salts which are aluminosilicate-like. However, Co<sup>2+</sup> ions have a strong tendency to form

<sup>⊗</sup> Abstract published in *Advance ACS Abstracts*, February 15, 1997.

(1) Breck, D. W. *Zeolite Molecular Sieves*; Wiley & Sons: New York, 1974.

(2) Gier, T. E.; Stucky, G. D. *Nature (London)* **1991**, *349*, 508.

(3) Wilson, S. T.; Lok, B. M.; Messina, C. A.; Cannan, T. R.; Flanigen, E. M. *J. Chem. Soc., Chem. Commun.* **1982**, *104*, 1146.

(4) Soghomonian, V.; Chen, Q.; Haushalter, R. C.; Zubieta, J.; O'Connor, C. J. *Science* **1993**, *259*, 1596–1599.

(5) Soghomonian, V.; Chen, Q.; Haushalter, R. C.; Zubieta, J. *Angew. Chem., Int. Ed. Engl.* **1993**, *32*, 610–612.

(6) Haushalter, R. C.; Mundi, L. A. *Chem. Mater.* **1992**, *4*, 31–48.

(7) Cheetham, G. M. T.; Harding, M. M.; Rizkallah, P. J.; Kaucic, V.; Rajic, V. *Acta Crystallogr.* **1991**, *C47*, 1361–1364.

(8) Rajic, N.; Logar, N.; Kaucic, V. *Zeolites* **1995**, *15*, 672–678.

(9) Lin, S. S.; Weng, H. S. *Appl. Catal.* **1993**, *A105*, 289.

(10) Dakka, J.; Sheldon, R. A. The Netherlands Patent 9,200,968, 1992.

(11) Chen, J.; Jones, R. H.; Natarajan, S.; Hursthouse, M. B.; Thomas, J. M. *Angew. Chem., Int. Ed. Engl.* **1994**, *33*, 639.

(12) Wilson, S. T.; Lok, B. M.; Messina, C. A.; Cannan, T. R.; Flanigen, E. M. In *Intrazeolite Chemistry*; Stucky, G. D., Dwyer, F. G., Eds.; ACS Symposium Series No. 218; American Chemical Society: Washington, DC, 1983; pp 79–118.

(13) *Inorganic Crystal Structure Database*, FIZ Karlsruhe and Gmelin-Institut, 1996.

Co–O–Co linkages and adopt the non-tetrahedral coordination such as trigonal bipyramidal<sup>15</sup> or octahedral<sup>16</sup> configurations.

In this report, we will describe our efforts to search for synthesis conditions which give rise to cobalt phosphate zeolite frameworks. Five tetrahedral cobalt phosphate framework structures which have chiral symmetry combined with a strict alternation of Co<sup>2+</sup> and P<sup>5+</sup> tetrahedra are reported here. The chiral symmetry exhibited by these materials is of particular interest as there has been much attention put into the preparation of chiral zeolite frameworks for potential applications involving enantioselective separation and catalysis.<sup>17,18</sup> RbCoPO<sub>4</sub> and the monoclinic polymorph of NH<sub>4</sub>CoPO<sub>4</sub>, both of which crystallize in *P*2<sub>1</sub>, are the only pure cobalt phosphates with a known zeolite topology (Li-ABW in this case).<sup>19,20</sup> The three other salts have hexagonal symmetry. Crystals of KCoPO<sub>4</sub> and the hexagonal polymorph of NH<sub>4</sub>CoPO<sub>4</sub> crystallize in *P*6<sub>3</sub> while crystals of NaCoPO<sub>4</sub> crystallize in *P*6<sub>1</sub>, which is a subgroup of *P*6<sub>3</sub>. This work thus represents a first step toward a rational design of pure microporous cobalt phosphate materials.

## Experimental Section

**A. Synthesis. 1. NaCoPO<sub>4</sub>.** CoCO<sub>3</sub>·*x*H<sub>2</sub>O (1.13 g) was mixed with 16.1 g of distilled water. Carbon dioxide evolved when 1.97 g of 85% H<sub>3</sub>PO<sub>4</sub> was slowly added to the above mixture. The mixture was then titrated with a 6 M NaOH solution to a pH value of 9.95 as measured using a Ag/AgCl electrode pH meter. A total of 4.50 mL of NaOH solution was added. The mixture was heated at 180 °C for 4 days in a Teflon-coated steel autoclave. The product was recovered by filtration and washed with deionized water. Dark-blue needle-like crystals were obtained from a mixture which also consisted of red needle-like crystals as a minor phase. The red phase has been identified as another polymorph of NaCoPO<sub>4</sub> with Co<sup>2+</sup> cations in the trigonal bipyramidal coordination.<sup>15</sup> The relative amount of the blue phase was drastically reduced when the pH of the solution was lowered or increased by 1. The pure blue phase could be obtained by heating the mixture to a temperature of 925 °C at which the red phase transformed into the blue phase.<sup>16</sup>

**2. KCoPO<sub>4</sub>.** CoCO<sub>3</sub>·*x*H<sub>2</sub>O (1.40 g) was mixed with 20.0 g of distilled water. Carbon dioxide evolved when 2.45 g of 85% H<sub>3</sub>PO<sub>4</sub> was slowly added to the above mixture. The mixture was then titrated with a 6 M KOH solution to a pH value of 8.10 as measured using a Ag/AgCl electrode pH meter. A total of 5.24 mL of KOH solution was added. The mixture was heated at 150 °C for 4 days in a Teflon-coated steel autoclave. The product was recovered by filtration and washed with deionized water. Thin blue needle crystals of KCoPO<sub>4</sub> were obtained. The largest dimension of these crystals was about 150 μm. The syntheses performed at other pH values ranging from 7.1 to 10.2 gave the same blue KCoPO<sub>4</sub> phase. Much larger, chunky crystals up to 1 mm in size could be obtained if a small amount of an amine such as ethylenediamine was added into the synthesis mixture. When the relative amount of ethylenediamine was increased, large crystals of CoPO<sub>4</sub>·<sup>1</sup>/<sub>2</sub>C<sub>2</sub>H<sub>4</sub>(NH<sub>3</sub>)<sub>2</sub><sup>11</sup> were grown.

**3. NH<sub>4</sub>CoPO<sub>4</sub>-HEX.** CoCO<sub>3</sub>·*x*H<sub>2</sub>O (0.78 g) was added to 1.44 g of 85% H<sub>3</sub>PO<sub>4</sub>. Carbon dioxide evolved and the mixture was stirred for about 5 min. Ethylene glycol (17.78 g) was then added to the above mixture with stirring. The pH of the solution was adjusted to 7.50 with 29.9% NH<sub>4</sub>OH solution using a Ag/AgCl electrode pH meter. Since the pH value was measured in an ethylene glycol environment, it might not be directly comparable with measurements obtained from

an aqueous solution. After being aged for 1 h at room temperature, the gel was transferred to a 60-mL Teflon-coated steel autoclave and heated at 180 °C for 12 days. Vivid blue crystals of NH<sub>4</sub>CoPO<sub>4</sub> were prepared in high purity. The largest dimension of crystals was about 30 μm. No blue phases could be obtained when the pH of the solution was increased by 1 whereas a mixture of two blue phases (hexagonal and ABW) and an unidentified pink phase were observed when the pH was dropped to 6.4.

**4. NH<sub>4</sub>CoPO<sub>4</sub>-ABW.** CoCO<sub>3</sub>·*x*H<sub>2</sub>O (0.58 g) was added to 1.07 g of 85% H<sub>3</sub>PO<sub>4</sub>. Carbon dioxide evolved and the solution was stirred for about 5 min. Ethylene glycol (13.34 g) was then added to the above mixture with stirring. The pH of the solution was adjusted to 9.00 with 1,4-diaminobutane. The gel was heated at 180 °C for 12 days in a 23-mL Teflon-coated steel autoclave. Vivid blue crystals of NH<sub>4</sub>-CoPO<sub>4</sub> were prepared in high purity. The largest dimension of crystallites was about 60 μm.

**5. RbCoPO<sub>4</sub>.** CoCO<sub>3</sub>·*x*H<sub>2</sub>O (2.04 g) was added to 7.26 g of distilled H<sub>2</sub>O. H<sub>3</sub>PO<sub>4</sub> (4.20 g, 85%) was slowly added to the above solution. The pH of the solution was adjusted to 8.29 with 50 wt % RbOH solution. A total of 13.61 g of RbOH solution was added. The mixture was divided into two parts, both of which were heated for 8 days in two separate Teflon-coated steel autoclaves at temperatures of 150 and 180 °C, respectively. Vivid blue powders of RbCoPO<sub>4</sub> were prepared in high purity. The products from the two batches were the same according to their powder diffraction patterns. The syntheses performed at other pH values ranging from 5.7 to 8.9 gave the same blue RbCoPO<sub>4</sub> phase.

**B. Elemental Analysis and Thermal Analysis.** The elemental analyses were performed by Microanalytical Laboratory (University of California, Berkeley) on samples of NH<sub>4</sub>CoPO<sub>4</sub>-HEX and NH<sub>4</sub>-CoPO<sub>4</sub>-ABW. The calculated values (in mass percent) were 8.15 N and 2.34 H for both samples; experimental values were 7.89 N, 2.53 H for NH<sub>4</sub>CoPO<sub>4</sub>-HEX and 7.97 N, 2.47 H for NH<sub>4</sub>CoPO<sub>4</sub>-ABW.

The NH<sub>4</sub>CoPO<sub>4</sub>-ABW phase was analyzed with thermogravimetric analysis (TG) and differential thermal analysis (DTA) which were performed on a Netzsch Simultaneous Thermal Analysis (STA) 409 system in static air with a heating rate of 5 °C/min from 30 to 950 °C using a sample weight of 50.0 mg. Between 260 and 460 °C, there was a broad one-step weight loss of 15.3% accompanied by an endothermic peak. The observed weight loss agreed with the calculated value of 15.1% for the loss of half of a water molecule and one ammonia molecule (NH<sub>4</sub>CoPO<sub>4</sub> → NH<sub>3</sub> + <sup>1</sup>/<sub>2</sub>H<sub>2</sub>O + <sup>1</sup>/<sub>2</sub>Co<sub>2</sub>P<sub>2</sub>O<sub>7</sub>). The residue recovered from 800 °C was identified as Co<sub>2</sub>P<sub>2</sub>O<sub>7</sub> by X-ray powder diffraction.

**C. Magnetic Susceptibility.** Susceptibility measurements were carried out using a Quantum Design MPMS-5S Magnetic Properties Measuring System. Samples consisted of 3–16 mg of MCoPO<sub>4</sub> suspended in 8–12 mg of Sticast 1266 epoxy. Accurate sample weights were determined by thermogravimetric analysis of the pellets after completion of the susceptibility measurements. Data were collected over the temperature range of 1.7–300 K with an applied field of 250 G.

**D. X-ray Crystallography.** A summary of crystal data and refinement results for NaCoPO<sub>4</sub>, KCoPO<sub>4</sub>, NH<sub>4</sub>CoPO<sub>4</sub>-HEX, NH<sub>4</sub>-CoPO<sub>4</sub>-ABW, and RbCoPO<sub>4</sub> is provided in Table 1.

**1. NaCoPO<sub>4</sub> and KCoPO<sub>4</sub>.** An ORTEP diagram for NaCoPO<sub>4</sub> is shown in Figure 1. Its racemic twinning leads to no complication in the structural analysis. The structural studies of KCoPO<sub>4</sub>, on the other hand, were complicated by the pseudosymmetry and twinning. A single crystal of KCoPO<sub>4</sub> was initially examined on a Huber 4-circle diffractometer. The structure was solved and refined in a hexagonal cell (*a* = 10.5136(4) Å, *c* = 8.5203(3) Å) with *P*6<sub>3</sub> space group. The resulting *R*-factor was 7.95% with some oxygen atoms having elongated thermal ellipsoids.

A second study on the same crystal was done on a Siemens Smart CCD diffractometer. A hexagonal cell with a triple volume was found with *a* = 18.230(1) Å and *c* = 8.5208(7) Å.<sup>21</sup> The refinement in the supercell was done in the same space group (*P*6<sub>3</sub>) and showed no improvement over the refinement done in the subcell. Significant improvements in both subcell and supercell could be made, however, by assuming that the crystal was twinned.<sup>22</sup>

Powder XRD was used to confirm the supercell structure of this compound. Two supercell reflections were detected with relative

(14) Lowenstein, W. *Am. Mineral.* **1954**, *39*, 92.

(15) Feng, P. Y.; Bu, X. H.; Stucky, G. D. *J. Solid State Chem.* In press.

(16) Feng, P. Y.; Bu, X. H.; Stucky, G. D. *J. Solid State Chem.* Submitted for publication.

(17) Davis, M. E. *Acc. Chem. Res.* **1993**, *26*, 111–115.

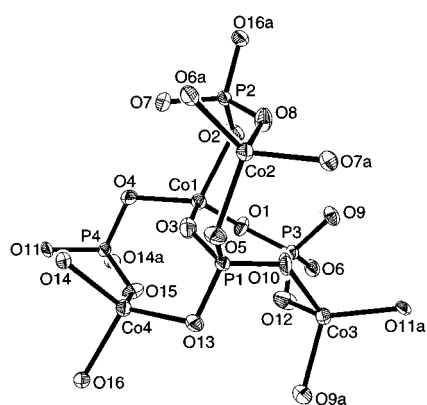
(18) Bruce, D. A.; Wilkinson, A. P.; White, M. G.; Bertrand, J. A. *J. Solid State Chem.* **1996**, *125*, 228.

(19) Meier, W. M.; Olsen, D. H. *Atlas of Zeolite Structure Types*; Butterworths: Washington, 1992.

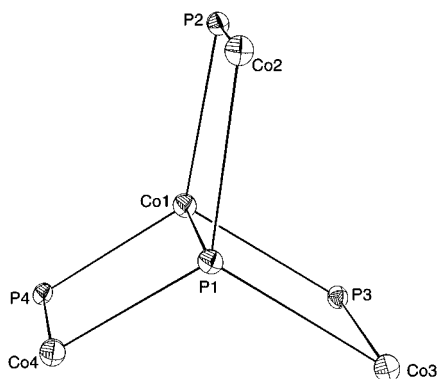
(20) While this manuscript was under review, we noticed that a reference on RbCoPO<sub>4</sub> was given in the updated version of the following: *Atlas of Zeolite Structure Types*; Elsevier: New York, 1996. Rakotomahanina Ralaisoa, E. L. Dissertation, University of Grenoble, 1972.

**Table 1.** Crystal Data and Refinement Summaries for NaCoPO<sub>4</sub>, KCoPO<sub>4</sub>, NH<sub>4</sub>CoPO<sub>4</sub>-HEX, NH<sub>4</sub>CoPO<sub>4</sub>-ABW, and RbCoPO<sub>4</sub>

formula	NaCoPO <sub>4</sub>	KCoPO <sub>4</sub>	NH <sub>4</sub> CoPO <sub>4</sub> -HEX	NH <sub>4</sub> CoPO <sub>4</sub> -ABW	RbCoPO <sub>4</sub>
fw	176.89	193.01	171.94	171.94	239.37
habit	hexagonal prism	thin needle	hexagonal prism	bipyramid	powder
color	blue	blue	blue	blue	blue
size (μm <sup>3</sup> )	230 × 83 × 83	250 × 33 × 33	25 × 25 × 38	40 × 54 × 54	
<i>a</i> (Å)	10.1918(1)	18.230(1)	10.7189(6)	8.7968(7)	8.8377(8)
<i>b</i> (Å)	10.1918(1)	18.230(1)	10.7189(6)	5.4621(4)	5.4150(5)
<i>c</i> (Å)	23.9013(1)	8.5208(7)	8.7096(6)	9.0105(7)	8.9723(8)
$\beta$	90	90	90	89.983(2)	90.212(2)
<i>V</i> (Å <sup>3</sup> )	2150.08(3)	2452.4(3)	866.62(9)	432.95(6)	429.38(6)
<i>Z</i>	24	24	8	4	4
space group	<i>P</i> 6 <sub>1</sub> (No. 169)	<i>P</i> 6 <sub>3</sub> (No. 173)	<i>P</i> 6 <sub>3</sub> (No. 173)	<i>P</i> 2 <sub>1</sub> (No. 4)	<i>P</i> 2 <sub>1</sub> (No. 4)
$\lambda$ (Å)	0.71073	0.71073	0.71073	0.71073	1.5418
$\mu$ (mm <sup>-1</sup> )	5.208	5.480	4.221	4.224	49.716
$\rho_{\text{calc}}$	3.279	3.136	2.636	2.638	3.703
2 $\theta_{\text{max}}$ (deg)	56.46	55.98	41.76	55.96	100
no. of unique data	3486	3864	508	1916	4200
parameters	255	255	57	131	58
<i>R</i> ( <i>F</i> ) (%)	2.87	3.32	6.15	4.56	4.67 ( <i>R</i> <sub>p</sub> )
<i>R</i> <sub>w</sub> ( <i>F</i> <sup>2</sup> ) (%)	6.33	6.35	13.0	9.47	6.00 ( <i>wR</i> <sub>p</sub> )
GOF	1.08	1.17	1.22	1.16	2.02 ( $\chi^2$ )



(a)



(b)

**Figure 1.** NaCoPO<sub>4</sub>: The [2.2.2]propellane-like triple four-ring unit serving as the structural building block. (a) ORTEP view with bridging oxygen atoms; (b) tetrahedral atom connectivity diagram with oxygen atoms omitted for clarity. Atom labels having "a" refer to symmetry-generated atoms.

intensity equal to about 2% of that of the strongest peak. These two peaks occur at 29.97° and 31.57° in  $2\theta$  and were not indexable with the subcell, but could be indexed as (4 2 0) and (5 1 0) with the supercell.

(21) A brief description of the crystal structure of KCoPO<sub>4</sub> with nearly the same structure was reported. The crystal was prepared under a different condition. Lugaan, M.; Kubel, F.; Schmid, H. *Z. Naturforsch.* **1994**, *49B*, 1256–1262.

(22) The merging *R*-factor of the raw data (without absorption correction) in *6/mmm* is 10.5% as compared to 4.4% in *6/m*. This suggests that the crystal is twinned to give an approximate higher Laue symmetry.

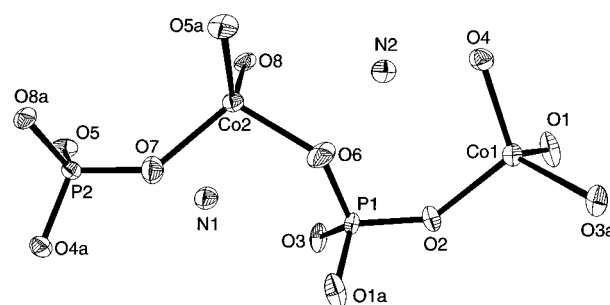


**Figure 2.** The ORTEP view of tetrahedral coordination environments for Co and P in the asymmetric unit of NH<sub>4</sub>CoPO<sub>4</sub>-ABW. Atom labels having "a" refer to symmetry-generated atoms.

**2. NH<sub>4</sub>CoPO<sub>4</sub>-HEX.** The initial identification of NH<sub>4</sub>CoPO<sub>4</sub>-HEX was made using X-ray powder diffraction data. It could be indexed in a hexagonal cell with  $a = 10.716(5)$  Å and  $c = 8.716(5)$  Å, which indicated that NH<sub>4</sub>CoPO<sub>4</sub>-HEX was isostructural to the subcell structure of KCoPO<sub>4</sub>. One important difference between powder diffraction patterns of KCoPO<sub>4</sub> and NH<sub>4</sub>CoPO<sub>4</sub>-HEX, however, was the absence of supercell reflections in NH<sub>4</sub>CoPO<sub>4</sub>-HEX data. No supercell reflections were observed in the subsequent single crystal studies of NH<sub>4</sub>CoPO<sub>4</sub>-HEX either. The structural parameters of KCoPO<sub>4</sub> obtained in a subcell were used as the starting model for the Rietveld refinement of NH<sub>4</sub>CoPO<sub>4</sub>-HEX. The single crystal studies of NH<sub>4</sub>CoPO<sub>4</sub>-HEX were subsequently done with the availability of very small twinned crystals.

**3. NH<sub>4</sub>CoPO<sub>4</sub>-ABW.** The structural analysis of NH<sub>4</sub>CoPO<sub>4</sub>-ABW was made difficult by twinning and the associated pseudo-orthorhombic symmetry. The intensity data gave orthorhombic symmetry with a merging *R*-factor of 4.44% as compared with 3.47% in monoclinic symmetry. However, the attempts to solve the structure in orthorhombic space groups were unsuccessful. It was suspected that NH<sub>4</sub>CoPO<sub>4</sub>-ABW might be monoclinic, but twinned so that it appeared to be orthorhombic. The structure was then solved in *P*2<sub>1</sub> and satisfactorily refined. An ORTEP diagram is shown in Figure 2.

**4. RbCoPO<sub>4</sub>.** RbCoPO<sub>4</sub> could only be prepared in the polycrystalline form. Its initial identification was achieved by comparing its powder diffraction pattern with that simulated from the structure of NH<sub>4</sub>CoPO<sub>4</sub>-ABW with the rubidium atomic scattering factor replacing that of the nitrogen atom. The Rietveld refinement used the structural parameters of NH<sub>4</sub>CoPO<sub>4</sub>-ABW as the initial model. The final observed, calculated, and difference X-ray powder diffraction patterns are shown in Figure 3.

## Results and Discussion

**A. Synthesis Conditions. 1. Synthesis.** The crystallization processes of cobalt phosphate salts reported here are very sensitive to the pH value of the gel solution. Some insight into

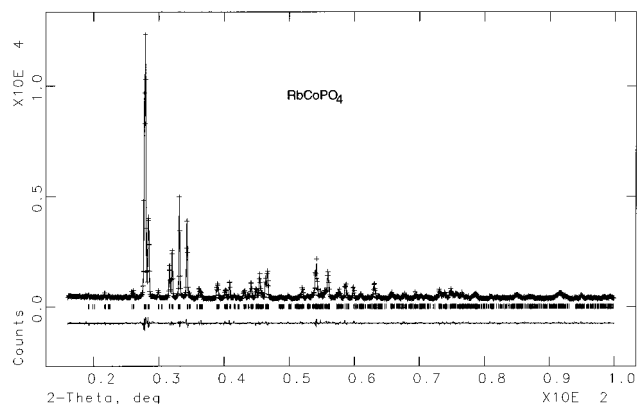


**Figure 3.** The final observed, calculated, and difference profiles for the X-ray Rietveld refinement for RbCoPO<sub>4</sub>.

both the structural stability of these compounds and the effect of varying chemical conditions can be gained by examining trends in synthesis conditions with variation in cation size. Crystals of KCoPO<sub>4</sub> are relatively easy to prepare and can be made in a relatively wide range of pH values. This suggests a good match between the K<sup>+</sup> cation size and the hexagonal CoPO<sub>4</sub> framework described here. This match produces a wide stability field for KCoPO<sub>4</sub>. In contrast, the preparations of NaCoPO<sub>4</sub> and the two phases of NH<sub>4</sub>CoPO<sub>4</sub> involve searching for the appropriate reaction conditions, pH, and solvent. These results suggest that both the smaller Na<sup>+</sup> ion and the larger NH<sub>4</sub><sup>+</sup> ion deviate from the ideal size for two CoPO<sub>4</sub> frameworks. This idea is confirmed by the observation that NaCoPO<sub>4</sub> can form in three different structures<sup>15,16</sup> and NH<sub>4</sub>CoPO<sub>4</sub> can be synthesized in two different structures, depending on the conditions. The fact that RbCoPO<sub>4</sub>, with the large Rb<sup>+</sup> cation, can be easily produced in the ABW structure in high purity further demonstrates this phenomena. ABW is apparently the stable framework for larger cations. This result offers promise for the future production of CoPO<sub>4</sub> frameworks with yet larger pores by the use of bigger cation templates.

By simple extrapolation, it could be argued that the pure tridymite structure should be the stable framework for the small Na<sup>+</sup> ion. This phase is not detected, however, and instead during the crystallization of NaCoPO<sub>4</sub>, a competing process which results in a red form of NaCoPO<sub>4</sub> is observed. This red color is indicative of non-tetrahedral Co<sup>2+</sup> ions. The relative amount of red and blue phases depends on the pH value. While this result confirms the general trend in stability with cation size discussed above, it also emphasizes that the correlations between the extra framework cation size and the framework type observed in MAISiO<sub>4</sub> (M is a monovalent cation) aluminosilicates<sup>23</sup> are not always found in CoPO<sub>4</sub> frameworks because of the large potential for non-tetrahedral bonding. CoPO<sub>4</sub> frameworks can more easily accommodate smaller ions by increasing the coordination number and thus the overall framework density than by changing the tetrahedral framework structure into a different topology. This option of increased coordination is not commonly available in aluminosilicate systems under similar reaction conditions.

A final note on synthesis conditions can provide additional insight into the stability of these compounds. Blue NaCoPO<sub>4</sub>, KCoPO<sub>4</sub>, and RbCoPO<sub>4</sub> were prepared from an aqueous solution. This is consistent with the observation that no hydrated forms of sodium, potassium or rubidium salts are known to exist. The two phases of the blue NH<sub>4</sub>CoPO<sub>4</sub>, however, were prepared in a predominantly non-aqueous environment as it was discovered that the presence of a large quantity of water gave rise to

a hydrated form, NH<sub>4</sub>CoPO<sub>4</sub>·H<sub>2</sub>O, in which Co<sup>2+</sup> has a non-tetrahedral coordination.<sup>24</sup> This result suggests that future work involving larger organic cations may also require predominantly non-aqueous environments to avoid non-tetrahedral Co<sup>2+</sup> coordination.

**2. Comparisons with Other Phosphates.** Zeolite analogues have been found in other divalent metal phosphates such as zinc- (or beryllio-) phosphates. Since the ionic radii<sup>25</sup> of tetrahedral Zn<sup>2+</sup> and Co<sup>2+</sup> are very close (0.60 Å for Zn<sup>2+</sup> and 0.58 Å for high-spin Co<sup>2+</sup>), cobalt phosphates often display similar structural properties as zinc phosphates. So far, however, significantly more successes have been achieved with zinc phosphates than with cobalt phosphates in the synthesis and characterization of open framework materials. For example, zeolite analogs of Li-ABW, sodalite, and zeolite-X are all known in zincophosphates whereas only the ABW phase is known in cobalt phosphates.

It is thus not surprising that three of the five cobalt phosphates (KCoPO<sub>4</sub>, RbCoPO<sub>4</sub>, and NH<sub>4</sub>CoPO<sub>4</sub>-ABW) reported here have structures isostructural to the corresponding zinc phosphates (KZnPO<sub>4</sub>,<sup>26</sup> RbZnPO<sub>4</sub>,<sup>27</sup> and NH<sub>4</sub>ZnPO<sub>4</sub>,<sup>28</sup>). A noted exception to this trend is found in NaCoPO<sub>4</sub>, which shows marked difference from NaZnPO<sub>4</sub>, the latter being derived from the beryllonite structure.<sup>29</sup> There are also four phases of LiZnPO<sub>4</sub><sup>30–32</sup> and three phases of CsZnPO<sub>4</sub>,<sup>33</sup> none of which have yet been discovered or characterized in the tetrahedral cobalt phosphate system.<sup>34</sup> It should be noted, however, that the same reactivity and structural variability which make Co<sup>2+</sup> useful for catalytic application is responsible for the difficulty in synthesizing tetrahedral CoPO<sub>4</sub> frameworks. The main group elements which show a stronger tendency toward simple tetrahedral bonding are observed in a much broader array of open framework structures.

**B. Structural Properties. 1. ABW Phases.** The NH<sub>4</sub>-CoPO<sub>4</sub>-ABW and RbCoPO<sub>4</sub> are the only pure cobalt phosphates with a framework topology (Figure 4) also found in aluminosilicate molecular sieves. The discovery of the CoPO<sub>4</sub>-ABW phases thus suggests that despite the unique coordination chemistry of Co<sup>2+</sup> cations, it is possible to make pure cobalt phosphate molecular sieves with aluminosilicate framework topologies. The inclusion of NH<sub>4</sub><sup>+</sup> in the CoPO<sub>4</sub>-ABW framework is interesting since the direct synthesis of ammonium zeolites is rare. The ammonium cations in zeolites are usually introduced by ion-exchange.<sup>35</sup>

The nitrogen atoms in the CoPO<sub>4</sub>-ABW channels are relatively close to the framework oxygen atoms with the closest distance of 2.83 Å for N1 and 2.86 Å for N2. This suggests the presence of hydrogen bonds. However, despite such directed hydrogen bonds, the NH<sub>4</sub><sup>+</sup> cations have more than one statistical orientation. All prominent residual electron density peaks

(24) Tranqui, D.; Duriff, A.; Guitel, J. C.; Averbuch-Pouchot, M. T. *Bull. Soc. Fr. Mineral. Cristallogr.* **1968**, *91*, 10–12.

(25) Shannon, R. D. *Acta Crystallogr.* **1976**, *A32*, 751–767.

(26) Andratschke, M.; Range, K.-J.; Haase, H.; Klement, U. *Z. Naturforsch.* **1992**, *47B*, 1249–1254.

(27) Elammari, L.; Elouadi, B. *J. Chim. Phys.* **1991**, *88*, 1969–1974.

(28) Bu, X. H.; Feng, P. Y.; Gier, T. E.; Stucky, G. D. To be submitted for publication.

(29) Elammari, L.; Durand, J.; Cot, L.; Elouadi, B. *Z. Kristallogr.* **1987**, *180*, 137–140.

(30) Bu, X. H.; Gier, T. E.; Stucky, G. D. *Acta Crystallogr.* **1996**, *C52*, 1601–1603.

(31) Harrison, W. T. A.; Gier, T. E.; Nicol, J. M.; Stucky, G. D. *J. Solid State Chem.* **1995**, *114*, 249–257.

(32) Bu, X. H.; Gier, T. E.; Stucky, G. D. To be submitted for publication.

(33) Blum, D.; Durif, A.; Averbuch-Pouchot, M. T. *Ferroelectrics* **1986**, *69*, 283–292.

(34) One salt, LiCoPO<sub>4</sub>, was known, but it is an octahedral cobalt salt. Kubel, F. *Z. Kristallogr.* **1994**, *209*, 755.

(35) Maher, P. K.; Hunter, F. D.; Scherzer, J. *Adv. Chem. Ser.* **1971**, *101*, 266–278.

(23) Liebau, F. *Structural Chemistry of Silicates*, Springer-Verlog: New York, 1985.

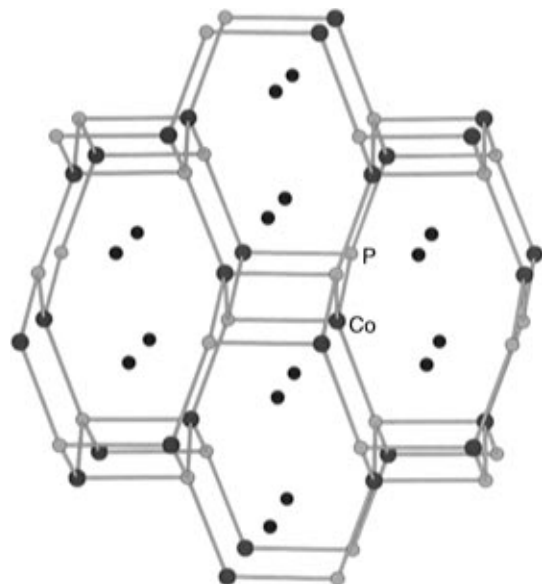


**Figure 4.**  $\text{NH}_4\text{CoPO}_4$ : The 8-ring channel in the ABW framework viewed along the  $b$ -axis. The hexagonal layers are stacked from left to right (the crystallographic  $a$ -axis). Four such layers are shown. Unconnected circles represent nitrogen atoms.

(protons) are located at a reasonable distance from the nitrogen atoms, but do not form a well-defined tetrahedra. This observation agrees with the correlation between the cation size and the framework topology discussed above and is an indication that  $\text{NH}_4^+$  cations are somewhat small for the  $\text{CoPO}_4$ -ABW type framework.

The poor match between the size of  $\text{NH}_4^+$  and the  $\text{CoPO}_4$ -ABW framework is further demonstrated through the study of two other ammonium ABW salts,  $\text{NH}_4\text{BePO}_4$  and  $\text{NH}_4\text{ZnPO}_4$ .<sup>28</sup> The  $\text{NH}_4^+$  cations in  $\text{NH}_4\text{ZnPO}_4$  are orientationally disordered just like  $\text{NH}_4^+$  in the cobalt salt. Replacing  $\text{Co}^{2+}$  or  $\text{Zn}^{2+}$  with smaller  $\text{Be}^{2+}$  ions (0.27 Å for  $\text{Be}^{2+}$ ) has the effect of compressing  $\text{ZnPO}_4$  or  $\text{CoPO}_4$  ABW frameworks. As a result,  $\text{NH}_4^+$  becomes a perfect match for the  $\text{BePO}_4$ -ABW framework. Such a perfect match is illustrated by the ordering of all four hydrogen atoms, all of which form strong hydrogen bonds with framework oxygen sites. These hydrogen atoms could be easily located from Fourier maps. The strong hydrogen bonding in  $\text{NH}_4\text{BePO}_4$  is also one reason that  $\text{NH}_4\text{BePO}_4$  has a higher thermal stability than either  $\text{NH}_4\text{CoPO}_4$  or  $\text{NH}_4\text{ZnPO}_4$ .

ABW type structures can be viewed as built from the stacking of layers with hexagonal rings (each ring has six tetrahedral atoms). The unit cells of the cobalt phosphate ABW phases are chosen so that the stacking direction is along the  $a$ -axis, just like in hydrated ABW structures with the standard orthorhombic setting. In hydrated aluminosilicate or zinco- (or beryllo-) phosphate or -arsenate ABW structures,<sup>2</sup> the repeat period along the layer stacking direction (10.313 Å in  $\text{LiAlSiO}_4 \cdot \text{H}_2\text{O}$ ) is usually more than 2 Å longer than the repeat period within the layer (8.194 Å in  $\text{LiAlSiO}_4 \cdot \text{H}_2\text{O}$ ).<sup>36</sup> In ammonium or rubidium cobalt phosphates, however, the repeat period along the layer stacking direction (8.797 Å for  $\text{NH}_4\text{-CoPO}_4$ -ABW) is actually slightly shorter than the repeat period within the layer (9.011 Å). This fact seems to suggest that the hexagonal layers in  $\text{CoPO}_4$ -ABW salts are much less corrugated than those in hydrated ABW frameworks.

**2. Hexagonal Phases.** The three hexagonal salts,  $\text{MCoPO}_4$  ( $\text{M} = \text{Na}^+, \text{K}^+, \text{NH}_4^+$ ), have essentially the same three-dimensional framework. This framework represents an intermediate structure between the tridymite and the ABW frame-

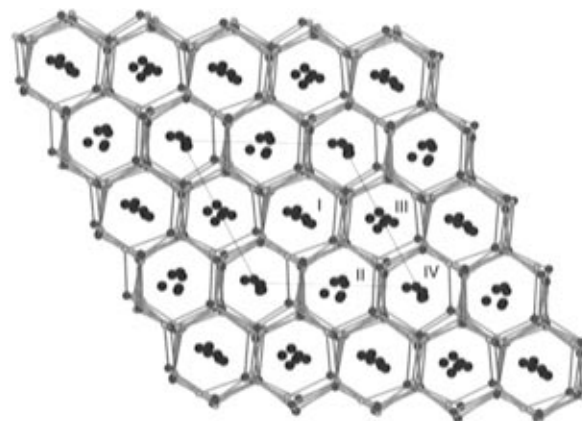


**Figure 5.**  $\text{NaCoPO}_4$ : Tetrahedral atom connectivity diagram showing the stacking of six crystallographic unique layers and six-ring channels along the  $c$ -axis. There are four different sodium distribution patterns corresponding to four unique channels.

works and has not been discovered in aluminosilicates and aluminophosphates. All three structures consist of hexagonal sheets stacked along the crystallographic  $c$ -axis. As in tridymite or zeolite Li-ABW type structures, the layers are eclipsed in projection and directly interconnected with oxygen bridges, thus forming continuous six-ring channels along the  $c$ -axis (Figure 5). The difference between tridymite or zeolite Li-ABW type structures and the hexagonal cobalt phosphate framework reported here is in the location of the bridging oxygens and associated puckering of the layers.

It is thus interesting to compare the hexagonal layer in hexagonal  $\text{MCoPO}_4$  phases with those previously discovered in aluminosilicates. In the hexagonal sheet one free corner of each tetrahedral atom can point up or down from the layer. Liebau and Barrer have systematically studied different ways in which the free corners of the tetrahedra point up or down in aluminosilicates. Barrer<sup>37</sup> listed four kinds of hexagonal sheets (Figure 6, a–d) found in zeolite minerals. Later Liebau<sup>23</sup> listed five different hexagonal sheets (Figure 6, a–c and e–f) found in  $\text{MAISiO}_4$  ( $\text{M} = \text{Li}^+, \text{Na}^+, \text{K}^+, \text{Rb}^+, \text{Cs}^+$ ) phases, two of which were not previously listed by Barrer. Of the six different sheets, only the tridymite type has a hexagonal cell. The sheet in the hexagonal  $\text{MCoPO}_4$  ( $\text{M} = \text{Na}^+, \text{K}^+, \text{NH}_4^+$ ) is different from any of these previously classified sheets and is shown in Figure 6g. Like tridymite, it also has a hexagonal cell, but with at least twice the translational periodicity (as in  $\text{NaCoPO}_4$ ,  $\text{NH}_4\text{-CoPO}_4$ -HEX, and the subcell structure of  $\text{KCoPO}_4$ ) within the sheet due to the presence of two types of hexagonal rings. In one type of hexagonal rings tetrahedral atoms point up and down alternatively (UDUDUD) as in tridymite (Figure 7b). In the other type of hexagonal rings three adjacent tetrahedral atoms all are directed up while the other adjacent three are directed down (UUUUDD) (Figure 7a) as in zeolite Li-ABW. Thus the cobalt phosphate hexagonal framework can be viewed as a hybrid of tridymite and zeolite ABW frameworks.

**3. Structural Building Unit.** The framework of cobalt phosphate salts can be described with the secondary building unit (SBU) which is a term typically used to characterize zeolite frameworks. The primary building units are single  $\text{TO}_4$  tetrahedra. Secondary building units which can contain up to 16 tetrahedral atoms are derived assuming the entire framework is made up of one type of SBU only.<sup>20</sup> Here we demonstrate that the concept of the secondary building unit can be applied fruitfully to denser frameworks as well. The secondary structural building block of the hexagonal  $\text{MCoPO}_4$  ( $\text{M} = \text{Na}^+$ ,

(36) Anderson, E. K.; Ploug-Sorensen, G. Z. *Kristallogr.* **1986**, *176*, 67–73.

(37) Barrer, R. M. *Zeolites and Clay Minerals*; Academic Press: New York, 1978.

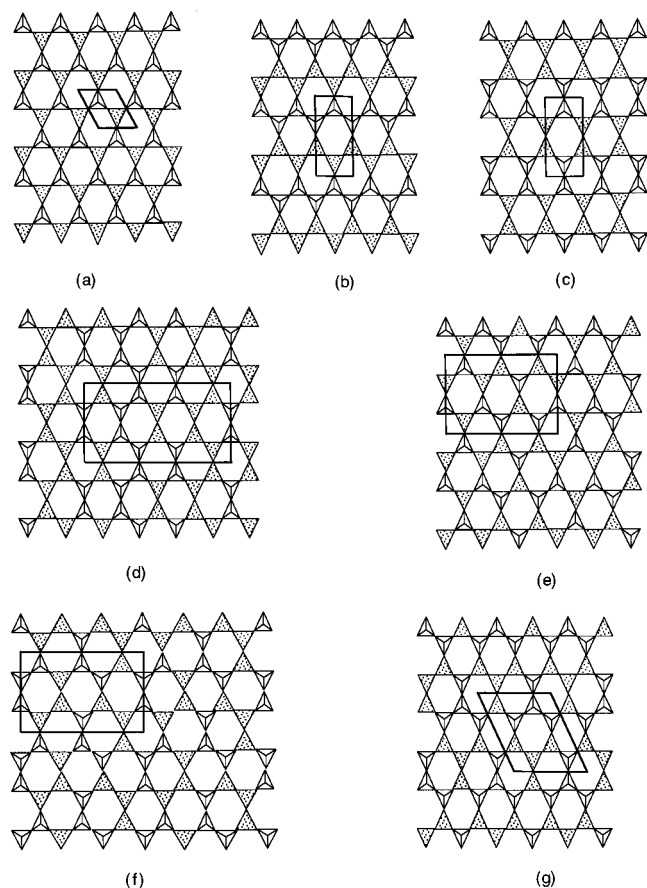


**Figure 6.** The seven different hexagonal layers. The type "d" occurs in mordenite and there is no direct connection between two hexagonal layers: (a) tridymite-type; (b) *Icmn*-type (ABW-type); (c) *Immm*-type; (e) beryllonite-type; (f) kaliophilite; (g)  $\text{NaCoPO}_4$ -type.

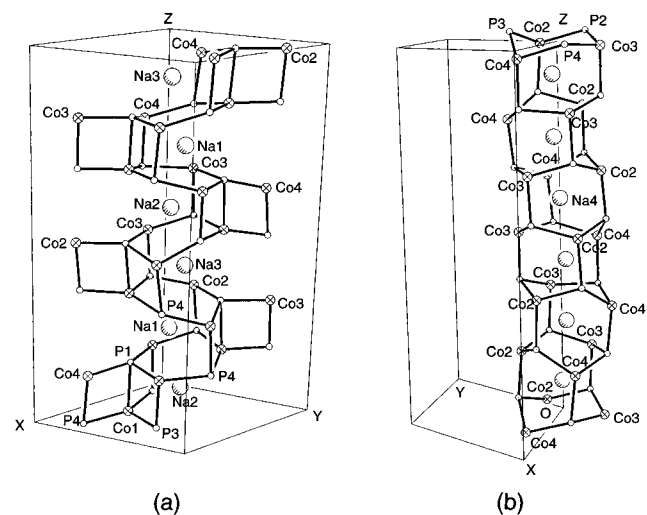


**Figure 7.**  $\text{NaCoPO}_4$ : Tetrahedral atom connectivity diagram showing two different six-ring channels. Only selected atoms are labeled. Unlabeled atoms have the same serial number as the atoms they are vertically (along *c*-axis) connected to. (a) The ABW portion of the framework (triple four-ring units are connected to form six-rings only); (b) the portion of the  $\text{NaCoPO}_4$  structure that resembles the stuffed tridymite.

$\text{K}^+$ ,  $\text{NH}_4^+$ ) framework is a triple four-ring unit like [2.2.2]-propellane (Figure 1). This unique structural building unit has not been found in zeolite structures for which at least 16 different secondary building units have been listed.<sup>20</sup>

The number of all possible framework structures that can be constructed from such a new secondary building block has not been derived. In theory, two such units can be connected to

create either new four-rings or six-rings. However, in the hexagonal structures reported here, the SBU's are joined in a manner so that only six-rings are formed (Figure 7a).

**4. Polymorphism.** In addition to the blue tetrahedral sodium cobalt phosphate, we have also discovered and characterized two other polymorphs of sodium cobalt phosphates. One polymorph which is slightly pink (nearly colorless) consists of octahedrally coordinated cobalt<sup>16</sup> while the other one which has a deep red color consists of trigonal bipyramidal cobalt.<sup>15</sup> In both pink and red phases, there are Co–O–Co linkages with trigonally coordinated oxygen atoms.

It is constructive to compare the three polymorphs of sodium cobalt phosphates with that of  $\text{SiO}_2$  and  $\text{AlPO}_4$ . The three commonly occurring polymorphs of  $\text{SiO}_2$  and  $\text{AlPO}_4$  (quartz-type, cristobalite-type, and tridymite-type) are all tetrahedral frameworks. While the tetrahedral sodium cobalt phosphate phase is structurally related to the tridymite-type, the other two cobalt phases adopt trigonal bipyramidal and octahedral coordinations, respectively, both of which have denser structures. The cobalt ion with its low valence has a great tendency to form edge-sharing polyhedra. These structures are usually unstable for high-charged species such as  $\text{Si}^{4+}$  because of increased electrostatic repulsion. Coordinations higher than four are also common for  $\text{Co}^{2+}$  at ambient conditions. Only at highly elevated pressures, typical of the earth's mantle, are octahedral silicate frameworks common.<sup>38</sup> These factors suggest that the crystallization of the desired microporous cobalt phosphates face competitions from a number of processes which are not usually encountered in the syntheses of aluminosilicate or aluminophosphate molecular sieves. Considerable efforts are needed to search for the suitable conditions for the synthesis of tetrahedral cobalt molecular sieves.

**5. Hexagonal Supercell Structures.** As the size of the extra framework cation increases, the unit cell expands in all three axial directions. The tripling of the *c*-axis in  $\text{NaCoPO}_4$ , which can be seen in Figure 7, gives rise to the subgroup symmetry of  $P6_1$ . As  $\text{Na}^+$  is replaced with  $\text{K}^+$ , the translational periodicity along the hexagonal *c*-axis is restored. This substitution, on the other hand, produces a loss of the periodicity parallel to the layer. The substitution with the larger  $\text{NH}_4^+$  cation restores the translational periodicity in directions both parallel and perpendicular to the hexagonal layers and produces the smallest possible cell which could be obtained from such kind of hexagonal layer. These details of superstructure demonstrate how the  $\text{CoPO}_4$  lattice can change to accommodate cations of different sizes.

It is interesting to note that the structural transition between subcell and supercell or between two supercells involves mainly the framework oxygen atoms. For example, the refinement result shows that the tetrahedral atoms in  $\text{KCoPO}_4$  could be very well described in the subcell. The appearance of supercell reflections upon the substitution of  $\text{NH}_4^+$  by  $\text{K}^+$  is apparently due to the increased ordering of oxygen atoms.

In  $\text{NaCoPO}_4$  and  $\text{KCoPO}_4$ , there is no point group symmetry imposed on the geometry of the triple four-ring unit. This is not the case, however, in the ammonium salt where the triple four-ring units have a 3-fold symmetry passing through the common axis of the triple four-ring unit. An important consequence is that the Co–O–P group on the 3-fold axis is linear ( $180^\circ$ ) by symmetry restriction. In comparison, the corresponding Co–O–P angles in  $\text{NaCoPO}_4$  and  $\text{KCoPO}_4$  are  $137.9(2)^\circ$  and  $162.9(4)^\circ$ , respectively. This gradual increase of the T–O–T angle from  $\text{Na}^+$  to  $\text{NH}_4^+$  illustrates the flexible nature of the  $\text{CoPO}_4$  framework. Such a large difference in T–O–T angles is also observed in aluminosilicates where the

(38) Hazen, R. M.; Downs, R. T.; Finger, L. W. *Science* **1996**, *272*, 1769.

**Table 2.** The Summary of Different Percentages of Twin Domains in Two Different Ammonium ABW Crystals, Two Different KCoPO<sub>4</sub> Crystals, and One Hexagonal Ammonium Crystal (Two Domains Related by the Twin Axis Have the Same Absolute Configuration. A Rotation and Racemic Twin Here is Equivalent to a Reflection Twin)

	component: A	rotation twin of A: B	racemic twin of A: C	rotation and racemic twin of A: D	enantiomorph ratio (A + B vs C + D)
NH <sub>4</sub> CoPO <sub>4</sub> -ABW (I) <sup>a</sup>	0.27(3)	0.24(3)	0.23(4)	0.26(3)	0.51:0.49
NH <sub>4</sub> CoPO <sub>4</sub> -ABW (II) <sup>b</sup>	0.11(5)	0.04(5)	0.67(6)	0.18(5)	0.15:0.85
KCoPO <sub>4</sub> (I) <sup>c</sup>	0.728(1)			0.272(1)	0.728:0.272
KCoPO <sub>4</sub> (II) <sup>d</sup>	0.299(5)	0.048(8)	0.63(1)	0.023(8)	0.347:0.653
NH <sub>4</sub> CoPO <sub>4</sub> -HEX	0.56(9)	0.03(8)	0.23(11)	0.18(8)	0.59:0.41

<sup>a</sup> Synthesized in the presence of 1,4-diaminobutane; refer to Table 1 for other structural information. <sup>b</sup> Synthesized together with the hexagonal phase in the presence of NH<sub>4</sub>OH. The main structural differences from "a" are the twin ratio listed here and the  $\beta$  angle (Table 3).  $R(F) = 5.37\%$ ,  $GOF = 1.07$  for 131 variables and 1227 reflections with  $I > 2\sigma(I)$ . <sup>c</sup> Synthesized without the presence of an amine; refer to Table 1 for other structural information. <sup>d</sup> Synthesized in the presence of ethylenediamine. The main structural difference from "c" is the twin ratio listed here.  $R(F) = 2.14\%$ ,  $GOF = 1.17$  for 257 variables and 3871 reflections with  $I > 2\sigma(I)$ .

Si—O—Si angle varies between ca. 120° and 180°. <sup>23</sup> The thermal parameter of the bridging oxygen in the common axis of the triple four-ring unit increases as the T—O—T angles increase from the Na<sup>+</sup> salt to the NH<sub>4</sub><sup>+</sup> salt ( $U_{eq} = 0.020(1) \text{ \AA}^2$  for O3 in NaCoPO<sub>4</sub>,  $U_{eq} = 0.045(2) \text{ \AA}^2$  for O3 in KCoPO<sub>4</sub>,  $U_{iso} = 0.058(9) \text{ \AA}^2$  for O6 in NH<sub>4</sub>CoPO<sub>4</sub>). This is in agreement with the observation that in aluminosilicates the thermal parameters of the oxygen atoms tend to increase as the Si—O—Si angle straightens. <sup>23</sup>

**6. Chirality and Twinning.** The structural similarities between these phases are emphasized by the fact that all phases have chiral symmetry. Chiral zeolites are of great importance because of their potential applications in both shape-selective and enantioselective separation and catalysis. One polymorph of zeolite  $\beta$  is an example of a zeolite structure with a chiral framework. The structure has been shown to have a 4-fold screw axis along the 12-ring channel (the 12-ring window is the largest pore opening in zeolite  $\beta$ ) in the *c*-direction. <sup>39</sup> This structural feature of zeolite  $\beta$  is shared by the cobalt phosphates reported here: for all of these new materials, the screw axes are along the direction of the channel system with the largest pore opening. For example, in the hexagonal CoPO<sub>4</sub> frameworks, the 6-fold screw axes are along the 6-ring channels which are the largest in these structures. In the CoPO-ABW frameworks, which have related 6-ring channels, the 2-fold screw axis is along the 8-ring channel instead of the 6-ring channel. Thus, even though crystallographically  $P2_1$  is a subgroup of  $P6_1$  and  $P6_3$ , the direction of the screw axis in these structures is coincident with the largest pore system and is not related to the supergroup—subgroup relationship.

The chiral structure of these cobalt phosphates is closely related to the twinning found in each material. Here, the structural differences among these cobalt phosphates are manifested in the fact that no two crystals were twinned the same way. The crystals of NaCoPO<sub>4</sub> were racemic twins (also called inversion twin) with 50% [the refined twin ratio = 0.51(1)] of each component. Racemic twinning similar to this also exists in other chiral materials such as NaZnPO<sub>4</sub>·H<sub>2</sub>O with  $P6_22$  symmetry. <sup>40</sup> The KCoPO<sub>4</sub> crystal synthesized without the use of an amine was a reflection twin in unequal volumes (Table 2). Such a twinning involved the exchange and reversal of the *a*- and *b*-axes and thus changed the absolute structure. However, there is an excess of one enantiomorph over the other [the enantiomorph ratio is 72.8% vs 27.2%]. A crystal of KCoPO<sub>4</sub> synthesized in the presence of ethylenediamine showed a significantly different twinning pattern. The single crystal structure analysis showed that the crystal was essentially an inversion twin (Table 2) with a dominating presence of the other

enantiomorph [the enantiomorph ratio is 34.7% vs 65.3%]. The crystal of NH<sub>4</sub>CoPO<sub>4</sub>-HEX was also twinned in unequal volumes (Table 2). It was a racemic twin as well as a reflection twin. The crystal of NH<sub>4</sub>CoPO<sub>4</sub>-ABW synthesized with 1,4-diaminobutane was a 50% racemic twin like NaCoPO<sub>4</sub> (Table 2). It was also rotation-twinned in equal ratio (Table 2). The rotation twinning involved the reversal of *b*- and *c*-axes and did not change the absolute configuration.

The existence of 50% racemic twins observed in some of these materials is generally considered to be an undesirable feature of chiral zeolites. As shown above for KCoPO<sub>4</sub>, we have found that the ratio of the two enantiomorphs can be significantly altered by changes in synthesis conditions. The similar effect was also found in the synthesis of NH<sub>4</sub>CoPO<sub>4</sub>-ABW crystals. The NH<sub>4</sub>CoPO<sub>4</sub>-ABW structure can be synthesized both as described above and by using NH<sub>4</sub>OH at a lower pH than that employed in the synthesis of the pure hexagonal phase. Single crystal diffraction on an ABW crystal synthesized from NH<sub>4</sub>OH showed that it was predominantly one enantiomorph (85% vs 15%). The detailed information on variation in twin ratios of the two ABW crystals is summarized in Table 2. <sup>41</sup> The ability to alter the ratio of chiral components through synthesis conditions and quantitatively characterize that ratio is of considerable importance for the application of chiral zeolite materials. We should note, however, that the change in ratio of the two enantiomorphs is based on a limited number of individual crystals and the results may not be representative of the bulk sample from which they were selected. A systematic study of a large number of randomly selected crystals is needed in order to gain a more complete understanding of the optical purity of bulk materials.

The different twinning ratio of the NH<sub>4</sub>CoPO<sub>4</sub>-ABW salts was also evidenced by the unit cell parameters, most notably, the  $\beta$  angle. The  $\beta$  angle of the 50% racemic and 50% rotation-twinned crystal was nearly exactly 90° [refined value = 89.983(2)°] as determined using the single crystal method. This angle deviated markedly from 90° when the volume ratios among twin domains were not equal [refined value = 90.305(2)° for 85% pure enantiomorph of NH<sub>4</sub>CoPO<sub>4</sub>-ABW]. Since no ABW crystals with only one completely pure enantiomorph phase were available, the X-ray Rietveld refinement of the powder sample was used to obtain a  $\beta$  angle free from the twinning effect. The results from powder data ( $\beta = 90.392(4)^\circ$ ) were in excellent agreement with the trend observed from single crystal methods. That is, there is an increasing angular deviation from 90° as an individual twin domain dominates the crystal (Table 3).

**C. Magnetic Susceptibility.** The pure tetrahedral arrangement of Co<sup>2+</sup> ions observed in X-ray diffraction can also be

(39) Newsam, J. M.; Treacy, M. M. J.; Koetsier, W. T.; de Gruyter, C. B. *Proc. R. Soc. London, A* **1988**, *420*, 375–405.

(40) Harrison, W. T. A.; Gier, T. E.; Stucky, G. D.; Broach, R. W.; Bedard, R. A. *Chem. Mater.* **1996**, *8*, 145–151.

(41) For a reference on the meaning of numbers in Table 2 refer to: *SHELXTL 5.0 Reference Manual*; Siemens Energy & Automation, Inc. Analytical Instrumentation; Chapter 9, p 10.

**Table 3.** Comparison of ABW Unit Cell Parameters Showing the Effect of the Twinning Ratio on the  $\beta$  Angle

	ratio between two enantiomorphs	<i>a</i>	<i>b</i>	<i>c</i>	$\beta$
NH <sub>4</sub> CoPO <sub>4</sub> (I)	51:49	8.7968(7)	5.4621(4)	9.0105(7)	89.983(2)
NH <sub>4</sub> CoPO <sub>4</sub> (II)	85:15	8.7882(11)	5.4589(7)	8.9958(11)	90.305(2)
NH <sub>4</sub> CoPO <sub>4</sub> (III)	powder <sup>a</sup>	8.7936(5)	5.4592(3)	9.0005(6)	90.392(4)

<sup>a</sup> The polycrystalline sample of (III) was ground from a batch of crystals from which the crystal (I) was picked.

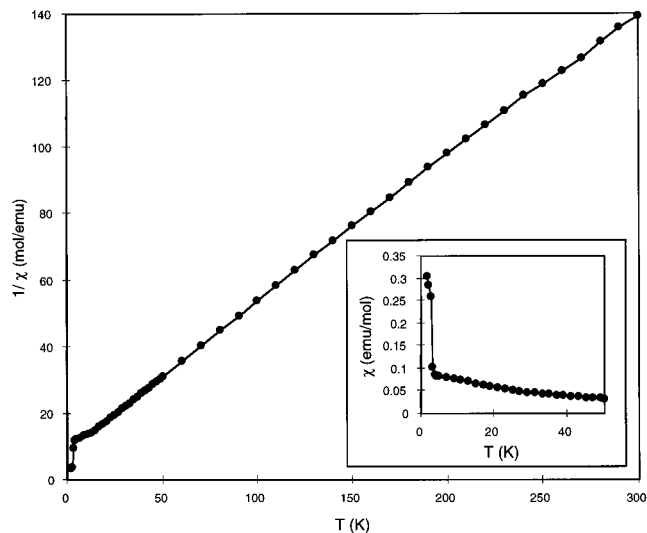


**Figure 8.** Molar magnetic susceptibility for NaCoPO<sub>4</sub> plotted as  $1/\chi$  versus  $T$ . Linear Curie–Weiss behavior is observed. The inset shows  $\chi$  versus  $T$  in the low-temperature regime demonstrating the onset of ferromagnetic ordering.

seen in the magnetic properties of these MCoPO<sub>4</sub> materials. Consistent with the predictions for tetrahedral Co<sup>2+</sup>, all of the compounds that were examined (NaCoPO<sub>4</sub>, KCoPO<sub>4</sub>, NH<sub>4</sub>-CoPO<sub>4</sub>-HEX, and NH<sub>4</sub>CoPO<sub>4</sub>-ABW, but not RbCoPO<sub>4</sub>) showed paramagnetic Curie–Weiss behavior with  $S = 3/2$  and a negative  $\theta$  value in the temperature range from 12 to 300 K (Figure 8).<sup>42</sup> Octahedral Co<sup>2+</sup> compounds tend to show  $S = 3/2$  susceptibility only in the high-temperature regime with effective  $S = 1/2$  behavior observed at lower temperature. Also in agreement with the predictions for pure tetrahedral Co<sup>2+</sup> compounds, the  $g$  values in the Na<sup>+</sup>, K<sup>+</sup>, NH<sub>4</sub><sup>+</sup>-HEX, and NH<sub>4</sub><sup>+</sup>-ABW compounds were 2.17, 2.44, 2.32, and 2.43, respectively. Significantly higher  $g$  values are typical of octahedral Co<sup>2+</sup>.<sup>43</sup>

In the temperature regime below 12 K, all samples show a positive deviation from simple Curie–Weiss behavior (i.e., an increase in magnetization is observed at low temperature). This increase can be assigned to the onset of ferromagnetic coupling in these material. Within the four compounds studied, there is a general trend of increasing transition temperature and magnitude with decreasing cation size. A sharp increase in susceptibility is observed around 3 K in NaCoPO<sub>4</sub> (Figure 8). In the closely related K<sup>+</sup> and NH<sub>4</sub><sup>+</sup>-HEX materials, this transition is not observed until below 2 K and the sharpness of the transition is dramatically reduced. In the NH<sub>4</sub>CoPO<sub>4</sub>-ABW material, only small deviations from the Curie–Weiss behavior are observed down to 1.7 K.<sup>44</sup> It should be noted that 3 K (NaCoPO<sub>4</sub>) is a very high ordering temperature for tetrahedral Co<sup>2+</sup> compounds which do not usually show ordering much above 1 K.<sup>45</sup> This comparatively high temperature is probably

(42) Carlin, R. L.; van Duijneveldt, A. J. *Magnetic Properties of Transition Metal Compounds*; Springer-Verlag: New York, 1977; pp 202–205.

(43) Abraham, A.; Pryce, M. H. L. *Proc. R. Soc. (London)* **1951**, A206, 173.

the result of effective superexchange interactions through the PO<sub>4</sub><sup>3-</sup> groups.<sup>46</sup> In agreement with this idea, the most compact structure (NaCoPO<sub>4</sub>) shows the highest ordering temperature.

## Conclusions

In this paper we have discussed the syntheses and characterizations of a new class of chiral tetrahedral cobalt phosphate compounds: MCoPO<sub>4</sub> ( $M = \text{Na}^+, \text{K}^+, \text{NH}_4^+, \text{Rb}^+$ ). These compounds can be synthesized under hydrothermal conditions by careful control of the solution pH and solvent. X-ray structural analysis shows that all five salts consist of purely tetrahedral Co<sup>2+</sup> in structures that are the same as or highly related to aluminosilicate tridymite and zeolite ABW. These materials include the only pure CoPO<sub>4</sub> salts with a known zeolite topology and thus mark an important first step toward the synthesis of CoPO<sub>4</sub> open framework materials currently observed predominantly in aluminosilicate and aluminophosphate materials. The chirality observed in all of these structures holds promise for potential enantioselective separation and catalysis applications. The discovery of such a series of salts with this exceedingly simple stoichiometry is also an enrichment to the solid state chemistry of Co<sup>2+</sup> species.

In contrast to MAISiO<sub>4</sub> ( $M = \text{Na}^+, \text{K}^+$ ) salts, however, which take several different framework topologies such as cristobalite, tridymite, and beryllonite, the framework topology of MCoPO<sub>4</sub> is quite similar for the Na<sup>+</sup>, K<sup>+</sup>, NH<sub>4</sub><sup>+</sup>, and Rb<sup>+</sup> salts presented above. This suggests that the cobalt phosphate frameworks described here are more flexible than aluminosilicate frameworks in accommodating cations of different sizes, either through framework distortion or the redistribution of oxygen atoms. Based on this idea, together with the fact that competing crystallization processes can lead to non-tetrahedral (trigonal bipyramidal or octahedral) cobalt phosphates rather than tetrahedral ones with significantly different topologies, we anticipate that the design of future tetrahedral cobalt phosphate open frameworks, while promising, will be somewhat difficult. We can, however, expect novel open framework topologies arising from a combination of tetrahedral, trigonal bipyramidal, and octahedral Co<sup>2+</sup>. The discovery of cobalt phosphates with the zeolite ABW structure illustrates that it is possible to make pure cobalt phosphate molecular sieves with a known zeolite topology.

**Acknowledgment.** This research was supported in part by the National Science Foundation under Grant DMR 95-20971.

**Supporting Information Available:** A detailed description of structural studies, figures showing the triple four-ring units in KCoPO<sub>4</sub> and NH<sub>4</sub>CoPO<sub>4</sub>-HEX, X-ray powder diffraction pattern for KCoPO<sub>4</sub>, and final observed, calculated, and difference profiles for the X-ray Rietveld refinement for NH<sub>4</sub>-CoPO<sub>4</sub>-HEX, and tables of positional coordinates, bond distances, and angles (45 pages). See any current masthead page for ordering and Internet access instructions.

JA9634841

(44) It is quite possible that the deviation from Curie–Weiss behavior observed in this case is due only to zero-field splitting and not to ferromagnetic ordering. Large zero-field splittings are common in tetrahedral Co<sup>2+</sup> compounds and can produce deviations from Curie–Weiss behavior of this magnitude.

(45) Moron, M. C.; Palacio, F.; Pons, J.; Casabo, J.; Carlin, R. L. *Eur. J. Solid State Inorg. Chem.* **1991**, 28, 431.

(46) Carlin, R. L. *Magnetochemistry*; Springer-Verlag: New York, 1986; p 305.